Pore water pressures in three dimensional slope stability analysis

Faradjollah Askari[1], **Orang Farzaneh**[2]

[1]Assistant professor, Geotechnical Earthquake Engineering Department, International Institute of Earthquake Engineering and Seismology, IIEES; Email: Askari@iiees.ac.ir

[2]Assistant professor, Civil Engineering Department, Engineering Faculty, University of Tehran; Email: ofarzane@chamran.ut. ac.ir

Abstract: *Although some 3D slope stability algorithms have been proposed in recent three decades, still role of pore pressures in three dimensional slope stability analyses and considering the effects of pore water pressure in 3D slope stability studies needs to be investigated. In this paper, a limit analysis formulation for investigation of role of the pore water pressure in three dimensional slope stability problems is presented. A rigid-block translational collapse mechanism is used, with energy dissipation taking place along planar velocity discontinuities. Results are compared with those obtained by others. It was found that water pressure causes the three-dimensional effects to be more significant, especially in gentle slopes. This may be related to the larger volume of the failure mass in gentle slopes resulting in more end effects. Dimensionless stability factors for three dimensional slope stability analyses are presented - including the 3D effect of the pore water pressure – for different values of the slope angle in cohesive and noncohesive soils.*

Keywords: *limit analysis, slopes, stability, three-dimensional, upper bound, pore water pressure.*

1. Introduction

Stability problems of slopes are commonly encountered in geotechnical engineering projects. Solutions of such problems may be based on the slip-line method, the limit-equilibrium method or limit analysis.

Although the limit-equilibrium method has gained a wide acceptance due to its simplicity, limit analysis takes advantage of the upper and lower bound theorems of plasticity theory and bound the rigorous solution of a stability problem from below and above.

The Effects of pore water pressure have been studied by Michalowski (1995) and Kim et al (1999) in 2D slope stability problems based on limit analysis method. In the study by Michalowski, pore water pressures, calculated using the pore-water pressure ratio ru, were regarded as external forces, and rigid body rotation along a log-spiral failure surface was used.

On the other hand, Kim et al (1999) used finite elements method to obtain the lower and upper bound solutions for slope stability problems.

Although some 3D slope stability algorithms have been proposed in recent decades, there are few researches considering the effects of pore water pressure in 3D slope stability studies (Chen and Chameau (1982) and Leshchinsky and Mullet (1988)). These methods are mainly based on limit equilibrium concepts.

In the framework of the limit state methods, the objective of this paper is to study the role of pore water pressures in three-dimensional slope stability problems using the upper-bound limit analysis method. The formulation on which the present research is based is an extension of the analysis method proposed by Farzaneh and Askari (2003).

2. Limit analysis method

The theorems of limit analysis (upper and lower bound) constitute a powerful tool to solve problems in which limit loads are to be found. The following assumptions are made in limit analysis method:

-The material is perfectly plastic

[Downloaded from ijce.iust.ac.ir on 2025-01-26]

- The limit state can be described by a yield function $f(\sigma_{ij})=0$, which is convex in the stress space σ_{ij}

- The material obeys the associated flow rule:

$$\dot{\varepsilon}_{ij}^{p} = \dot{\lambda}\frac{\partial f(\sigma_{ij})}{\partial \sigma_{ii}} \quad (1)$$

where:
$\dot{\varepsilon}_{ij}^{p}$ = plastic strain rate tensor of the soil
σ_{ij} = stress tensor
$\dot{\lambda}$ = a non-negative multiplier, which is positive when plastic deformations, occurs

Equation 1 is usually referred to as the normality rule.

Limit analysis takes advantage of the upper- and lower-bound theorems of plasticity theory to bound the rigorous solution to a stability problem from below and above. Limit analysis solutions are rigorous in the sense that the stress field associated with a lower-bound solution is in equilibrium with imposed loads at every point of the soil mass, while the velocity field associated with an upper-bound solution is compatible with imposed displacements. In simple terms, under lower-bound loadings, collapse is not in progress, but it may be imminent if the lower bound coincides with the exact collapse loading. Under upper bound loadings, collapse is either already underway or imminent if the upper bound coincides with the exact collapse loading. The range in which the true solution lies can be narrowed down by finding the highest possible lower-bound solution and the lowest possible upper-bound solution.

Theorems of limit analysis can be extended to analyze the stability problems in soil mechanics by modeling the soil as a perfectly plastic material obeying the associated flow rule.

The consequence of applying the normality condition to a frictional soil with an internal friction angle of ϕ will be a necessary occurrence of a volume expansion with an angle of dilatation $\psi=\phi$ during the plastic flow. In a large number of stability problems in soil mechanics such as slope stability, lateral earth pressure and bearing capacity problems, deformation conditions are not so restrictive and the soil deformation properties do not affect the collapse load largely (Davis-1968, Farzaneh and Askari-2003). Therefore, the adoption of the limit analysis approach and the associated flow rule in soils appears to be reasonably justified.

The approach used in this paper is based on the upper-bound theorem and can be used to find the safety factor of a slope. The form of the safety factor according to the definition given by Bishop (1955):

$$F = \frac{c}{c_m} = \frac{\tan\phi}{\tan\phi_m} \quad (2)$$

where c and ϕ are the real cohesion and internal friction angle of the material, and c_m and ϕ_m are the required magnitude of these parameters needed to maintain the equilibrium. Using Equation 2 in the upper bound formulation of the problem, one can obtain the safety factor instead of the limit load.

3. Formulation

The formulation used in this paper was originally proposed by Michalowski (1989) and improved by Farzaneh and Askari (2003) without consideration of pore water pressures. The formulation is a rigorous method, and lacks any simplifying assumption that may disturb the upper bound theorem. The approach used for the incorporation of the pore water pressures in this paper is the total weight approach in which the saturated weight of the soil is considered together with the pore water pressures along the contours of the soil mass.

Figures 1 and 2 show the failure mechanism used in this analysis. It consists of rigid translational blocks separated by planar velocity discontinuity surfaces. One or more surfaces can be used in each side of the blocks. Number of blocks and lateral surfaces of each block in the example shown in Figure 1 are four and three respectively. Analytical geometry relations used to compute

[Downloaded from ijce.iust.ac.ir on 2025-01-26]

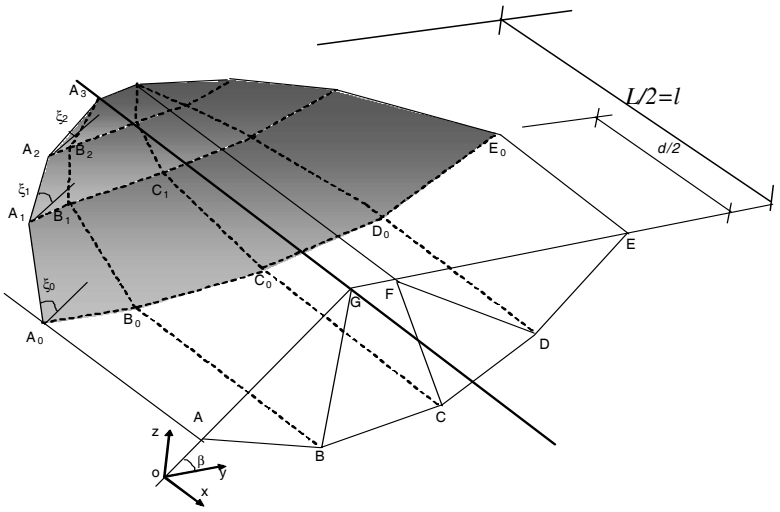

Fig. 1 Failure mechanism used in this analysis

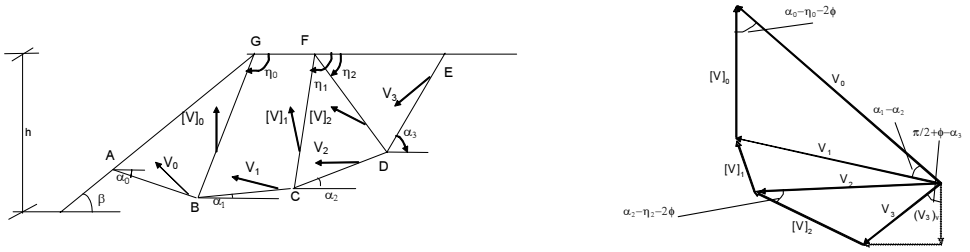

(a) (b)

Fig. 2 Collapse mechanism (a) cross-section in yoz plane; (b) hodograph

the areas and volumes of the blocks are similar to ones used by Farzaneh and Askari (2003). Using the hodograph shown in Figure 2(b), the velocities V_k of blocks (k = 0, 1... n-1; n is the number of blocks) and the velocity jumps between adjacent blocks $[V]_k$ can be derived (Appendix A). Having the velocities of all blocks, as well as their volumes and surface areas, one can write the energy balance equation in the following form:

$$\dot{W}_\gamma + \dot{W}_u = \dot{D} \tag{3}$$

where $\dot{W}_\gamma$ is the rate of work of block weights and $\dot{W}_u$ is the rate of work due to pore water pressure, regarded as an external force, and $\dot{D}$ is the energy dissipation rate in all the velocity discontinuities. Denoting the weight of block k as G_k, $\dot{W}_\gamma$ can be written as:

$$\dot{W}_\gamma = \sum_{k=1}^{n} G_k V_k \sin(\alpha_k - \varphi) \tag{4}$$

where n is the number of blocks, V_k is the velocity of block k,ϕ is the internal friction angle of the soil and α_k is the angle of the base of block k with horizon, as shown in Figure 2(a).

Having $\dot{w}_u$ on each surface discontinuity (described in Appendix B), the rate of energy due to pore water pressure in the collapse mechanism ($\dot{W}_u$) can be calculated as:

$$\dot{W}_u = -\sin\varphi\left(\sum_{k=1}^{n}\left(V_k\left(\int_{S_k} u dS\right)\right) + \sum_{k=1}^{n-1}\left([V]_k\left(\int_{[S]_k} u dS\right)\right)\right) \tag{5}$$

where S_k refers to the base and lateral surfaces of the block k, $[S]_k$ is the interface surface between blocks k and $k+1$, V_k is the velocity of block k, $[V]_k$ is the relative velocity between blocks k and $k+1$ and u is the pore water pressure distribution.

In the algorithm provided, pore water pressure distribution at the failure surfaces can be defined

[Downloaded from ijce.iust.ac.ir on 2025-01-26]

by any arbitrary function $u=u(x,y,z)$. In this paper, the function $u(x,y,z)$ has been introduced as follows:

1. by introducing a piezo surface ($u=\gamma_w.\ z_w$ where γ_w is the unit weight of water and z_w is the depth of the point below the piezo surface);

2. by considering a constant pore water pressure coefficient ($u=\ r_u.\gamma.z$, where γ is the total unit weight of the soil and z is the depth of the point below the soil surface).

Using the piezo surface or r_u, the value of pore water pressure at any point is determined. Integration of this function on any surface gives the pore water force on that surface.

$\int_{S_k} udS$ in Equation 5 is calculated by the following procedure:

- Surface S_k is subdivided into triangles S_{k1}, S_{k2}, …, S_{km}.

- Pore water pressure in a number of points on each triangle (S_{ki}) is determined as u_{ki1}, u_{ki2},…,u_{kim}. The number and location of these points can be chosen arbitrary depending on the precision needed. The procedure is explained briefly in the Appendix C.

Considering the average value of u_{ki1}, u_{ki2},…,u_{kim} as u_{ki} the pore water force on surface S_k is calculated as:

$$\int_{S_k} udS = \sum_{i=1}^{m} u_{ki} S_{ki} \tag{6}$$

The same procedure is used to calculate the integral $\int_{[S]_k} udS$.

The rate of energy dissipation per unit area of a velocity discontinuity surface for the Coulomb material can be written as $cV\cos\phi$ where V is the magnitude of the velocity jump vector. In the mechanism considered, the energy is dissipated along the block bases, sides and interfaces. With a reference to this assumption, the energy dissipation rate in the entire mechanism becomes

$$\dot{D} = c\cos\varphi\left(\sum_{k=1}^{n} S_k V_k + \sum_{k=1}^{n-1} [S]_k [V]_k\right) \tag{7}$$

Introducing c_m and ϕ_m from Equation 2 into Equations 4, 5 and 7 and using Equation 3, the following expression for the safety factor is obtained:

$$F = \frac{c_m \cos\varphi_m \left(\sum_{k=1}^{n} S_k V_k + \sum_{k=1}^{n-1} [S]_k [V]_k\right)}{\sum_{k=1}^{n} G_k V_k \sin(\alpha_k - \varphi_m) - \sin\varphi_m \left(\sum_{k=1}^{n} \left(V_k \left(\int_{S_k} udS\right)\right) + \sum_{k=1}^{n-1} \left([V]_k \left(\int_{[S]_k} udS\right)\right)\right)} \tag{8}$$

F in Equation (8) is implicit, because ϕ_m is equal to $tan^{-1}[(tan\ \phi)/F]$ in the right hand side of this Equation. It should be noted that the time for calculation of F by Eq. 8 is less than a minute.

The numerical technique used in the paper to find the set of α_k, η_k and ζ_k (Fig. 1) corresponding to the least upper-bound safety factor is the same as the procedure used by by Farzaneh and Askari (2003). In summary this technique is based on a simple two-step algorithm where in the first step, angles α_k, η_k and ζ_k are changed respectively twice by step $\Delta\alpha$($-\Delta\alpha$ and $+\Delta\alpha$) and the value of the safety factor is calculated after each change. If the variation causes a better result, the value of the respective angle is changed accordingly by $-\Delta\alpha$ or $+\Delta\alpha$. The calculations are continued until the results of two subsequent loops are the same. Step $\Delta\alpha$ is decreased in computations from 5^o to 0.1^o. In the second step, the procedure is followed by changing the values of the angles α_k, η_k and ζ_k simultanously, which is more convenient for solution of restricted (constrained) problems.

Using this optimization algorithm, the present method results have been compared with those of other investigators (such as Leschinsky (1992), Ugai (1985), Giger and Krizik (1976), Azzouz and Baligh (1975)). Almost in all cases, there was a good agreement between the results.

In the following sections, the computational results in two and three dimensional cases are discussed and compared with the other solutions. Then, typical numerical results are presented to demonstrate the importance of pore water pressure in 3D cases. Finally, dimensionless

[Downloaded from ijce.iust.ac.ir on 2025-01-26]

stability factors are presented for three different slope angles.

4. Comparison in 2-D Cases

For slopes, it is convenient to present the results of calculations in terms of the stability factor $\gamma h_c/c$ rather than the factor of safety. The stability factors calculated by present method for homogeneous slopes are compared with those obtained by Michalowski (1995) in Figure 3.

Calculations were performed assuming a collapse mechanism including 5 blocks. As mentioned above, The value of stability factor was sought in a minimization scheme considering angles α_k, η_k and ζ_k (Figures 1 and 2) and one of the lengths AG or EF as variable (Farzaneh & Askari, 2003). The pore pressure is expressed in terms of the coefficient r_u (defined as $u/\gamma h$ in section 3).

Figure 3 represents the stability factor as a function of slope angle (β) for r_u equal to 0.25 and 0.5. The results for ϕ =10°, 20° and 30° are presented on three separate diagrams and calculations were performed for β changing in 15° intervals. The results of both methods shown in Figure 3 follow each other very closely.

The influence of pore pressure is apparent by a reduction in stability factor $\gamma h_c/c$ with an increase in r_u. The adverse effect of the pore pressure increases by increasing of internal friction angle ϕ.

Kim et al (1999) obtained lower and upper bounds of the stability factors for simple slopes (Figure 4) in terms of effective stresses. In this analysis, three-nodded linear triangular finite elements were used to construct both statically admissible stress fields for lower-bound analysis and kinematically admissible velocity fields for upper-bound analysis.

Slopes with various inclinations were assumed on impervious firm bases with different depth factors. The soil strength parameters – the effective cohesion c' and the effective internal friction angle ϕ'– were assumed to be constant throughout the slope. Three values of friction angle (ϕ'=5, 15 and 25°) were assumed. To assess the effects of pore water pressure for various locations of the piezo surface, a number of situations were considered.

Kim et al (1999) checked the accuracy of Bishop's simplified method for slope stability analysis by comparing Bishop's solution (Bishop 1955) with lower- and upper-bound solutions. They also compared their results with factors of safety obtained from Janbu's stability charts (Janbu 1968) for a 45° slope. In Table 1 the results of the present study are compared with the results obtained by Kim et al for a 45° slope with D=2, H=10m, c′=20kN/m^2, γ =18kN/m^3 and for ϕ'=10° and 15°. The results are also compared with the factors of safety obtained from Janbu's stability charts (for ϕ'=15°) and simplified Bishop's solution, presented in the paper of Kim et al.

The results obtained by Kim et al are about 1% less (and accordingly better) than results obtained in the present analysis. As expected, factor of safety in all of the methods decreases as the water table rises. It is also observed that Janbu's stability chart gives conservative results in these cases, and Bishop's results are between those of lower and upper bounds. In general, good agreement is obtained between the present and the other solutions.

5. Comparison in 3-D Cases

Although the effect of pore water pressure has been considered in many 2D analyses, only few 3D solutions of this problem are available.

A general method of three dimensional slope stability analysis was proposed by Chen and Chameau (1982) using the limit equilibrium concept. The failure mass shown in Figure 5 was assumed symmetrical and divided into vertical columns. The inter-slice forces have the same inclination throughout the mass, and the inter-column shear forces were parallel to the base of

[Downloaded from ijce.iust.ac.ir on 2025-01-26]

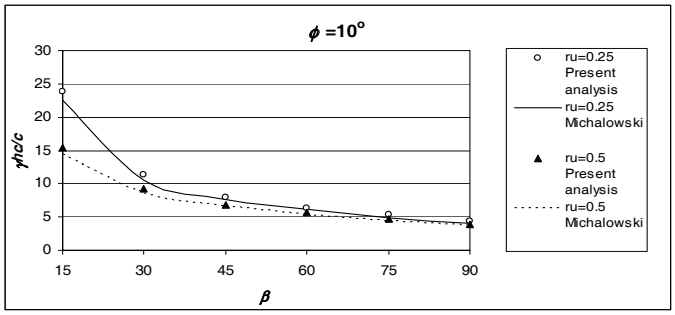

(a)

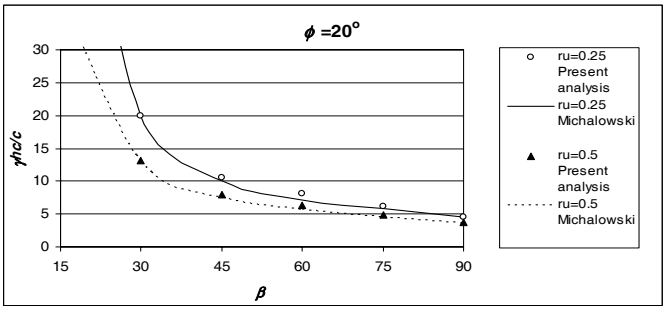

(b)

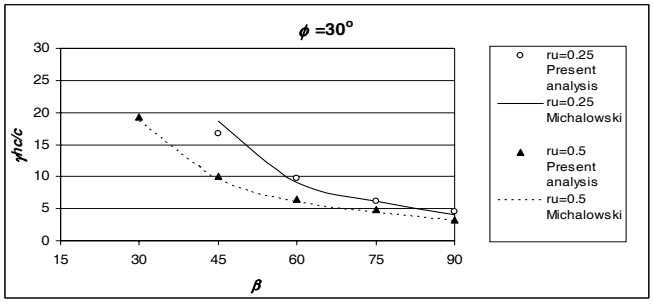

(c)

Fig. 3 Comparison of 2D stability factors of present analysis with those obtained by Michalowski (1995) for different slope angles; (a) ϕ =10º (b)ϕ =20º (c) ϕ =30º

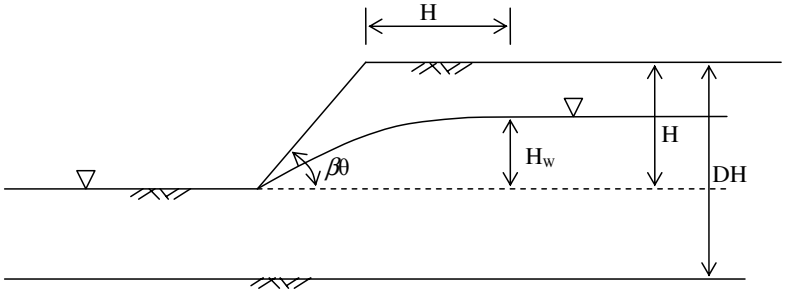

Fig. 4 Geometry of slope used in analysis by Kim et al (1999)

[Downloaded from ijce.iust.ac.ir on 2025-01-26]

Table 1 Comparison of 2D factor of safety for various conditions of water table (45° slope with D=2, H=10m, c'=20kN/m^2 and γ=18kN/m^3 for ϕ'=10° and 15° .

ϕ'	H_w(m)	Safety factor, F				
		Kim et al (lower-bound)	Kim et al (upper-bound	Bishop	Janbu's Chart	Present study
10°	2	0.96	1.05	0.99	_	1.06
	4	0.89	1.00	0.96	_	1.01
	6	0.83	0.89	0.92	_	0.96
15°	2	1.10	1.23	1.17	1.08	1.22
	4	1.04	1.17	1.10	1.03	1.17
	6	0.97	1.07	1.04	0.97	1.08

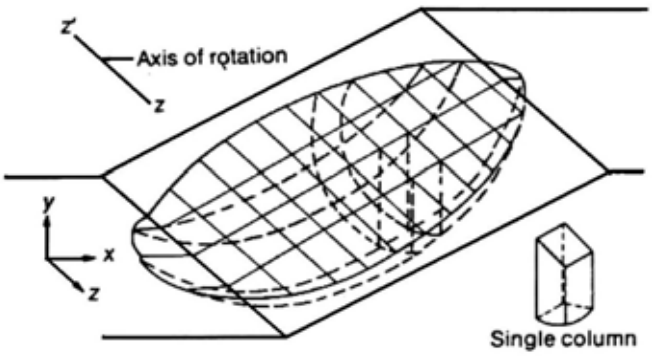

Fig 5 The failure mechanism in three dimensional method of slope stability proposed by Chen and Chameau (1982)

Table 2 Comparison of Ratio F3D/F2D with Chen and Chmeau (1982) for various Slope angles (c= 28.7 kPa, ϕ=1.5°, r_u= 0.5)

L/h	β (degree)	F_{3D}/F_{2D}	
		Chen and Chameau (1982)	Present study
3	16	1.29	1.21
	21.8	1.25	1.19
	33.7	1.14	1.14
5	16	1.14	1.13
	21.8	1.12	1.12
	33.7	1.07	1.08
7	16	1.1	1.1
	21.8	1.07	1.07
	33.7	1.04	1.05

[Downloaded from ijce.iust.ac.ir on 2025-01-26]

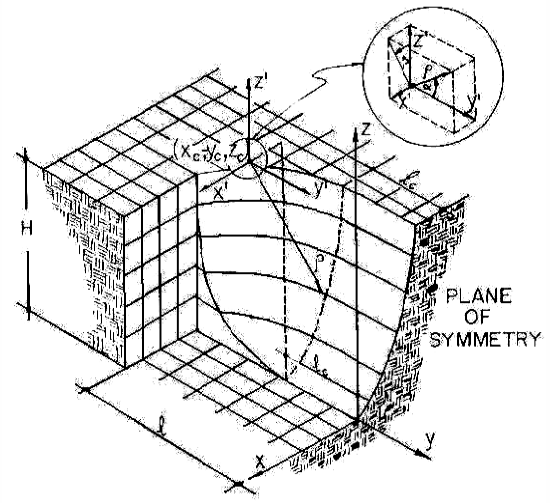

Fig. 6 The failure mechanism in 3D slope stability analysis of Leshchinsky and Mullet (1988)

the column and function of their positions. Force and moment equilibrium were satisfied for each column as well as for the total mass weight. In their paper, typical applications of this three dimensional model to slopes with different geometries and material properties were described.

Results of the present analysis are compared with Chen's for one case in Table 2. In this case, c'=28.7 kPa, ϕ'=1.5°, r_u=0.5, L/h=3, 5 and 7 (L: width of the mechanism) and β =16°, 21.8° and 33.7°. As can be seen, results of the two methods are very similar. In both methods, the ratio F_{3D}/F_{2D} decreases as β increases.

Leshchinsky and Mullet (1988) proposed a 3D slope stability procedure based on limit equilibrium method. The failure mechanism in their analysis, resulting from an analytical (variational) extremization procedure, is a 3D generalization of the log-spiral function. For this mechanism, shown in Figure 6, the moment limiting-equilibrium equation can be explicitly assembled and solved for the factor of safety.

Leshchinsky and Mullet have employed the following common nondimensional parameter:

$$\lambda = \frac{c'}{\gamma h \tan \phi'} \tag{9}$$

where h is the slope height.

Figure 7 shows a comparison between the results of Leschinsky's and present method. This diagram is prepared for vertical cuts, where the length of failure mechanism (L=2l) is known. The vertical axis is the minimum three dimensional safety factor with a given ru, divided by minimum two dimensional safety factor obtained with r_u=0. It should be pointed out that when r_u=0 are considered, safety factors obtained for two-dimensional cases are identical to those of Taylor (1937). Figure 7 shows that prediction by the present method compares favorably with Leschinsky's.

It must be mentioned that comparison of the results of the algorithm with the real cases or with those obtained from physical models tests was not possible due to lack of data in the literature for saturated soils.

6. Role of pore pressures in three dimensional slope stability analyses

Subsurface water movement and associated seepage pressures are the most frequent cause of slope instability. Subsurface water seeping toward the face or toe of a slope produces destabilizing forces, which can be evaluated by flow net. The piezometric heads, which occur along the assumed failure surface, produce outward forces that must be considered in the

[Downloaded from ijce.iust.ac.ir on 2025-01-26]

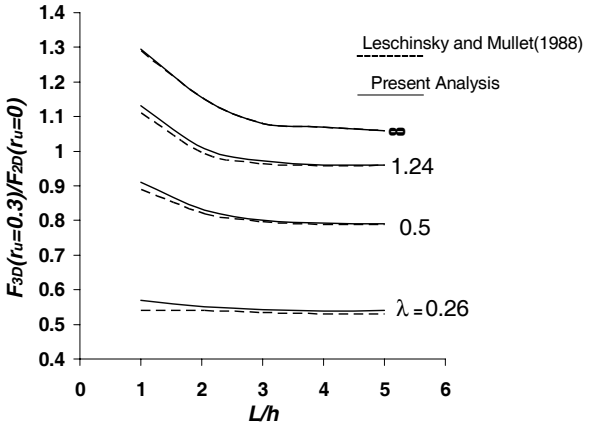

Fig.7 Comparison of results of Leschinsky and Mullet (1988) with present analysis

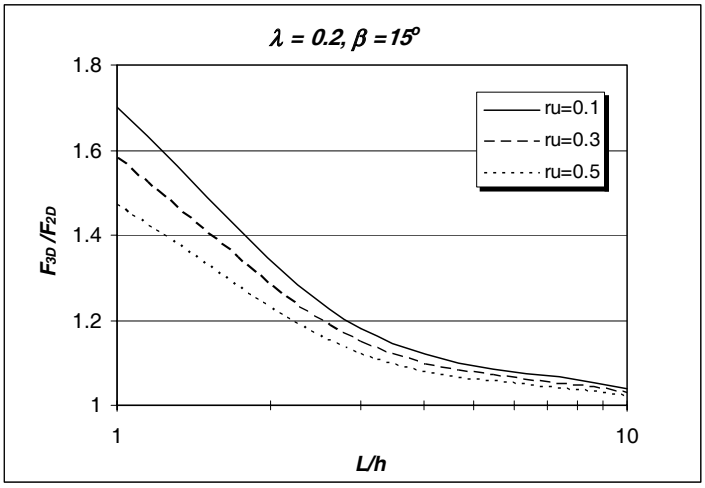

(a)

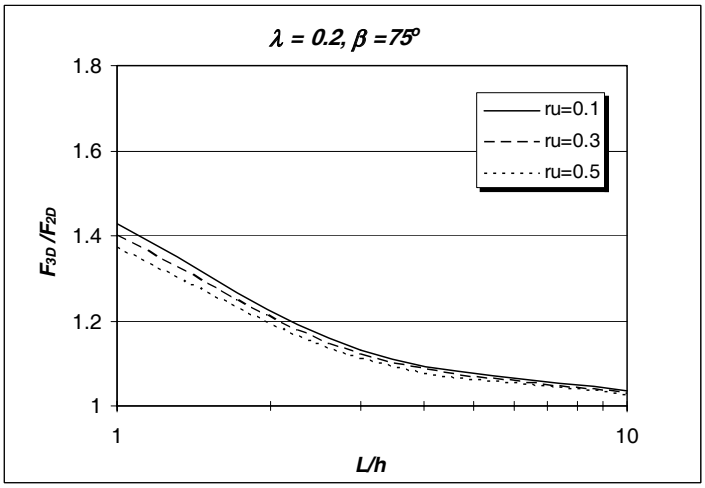

(b)

Fig. 8 Ratio F3D/F2D for two different values of slope angle β

[Downloaded from ijce.iust.ac.ir on 2025-01-26]

stability analysis.

When compressible fill materials are used in embankment construction, excess pore pressure may develop and must be considered in the stability analysis. Normally, field piezometric measurements are required to evaluate this condition. Where embankments are constructed over compressible soils, the foundation pore pressures must be considered in the stability analysis. Artesian pressures beneath slopes can have serious effects on the stability. Should such pressures be found to exist, they must be used to determine effective stresses and unit weights, and the slope and foundation stability should be evaluated by effective stress methods.

Most slope failure analyses are performed on a two dimensional model even though the shape of the slope failure in the field is truly three dimensional. Although few 3D slope stability algorithms have been proposed in recent three decades, still role of pore pressures in three dimensional slope stability analyses and considering the effects of pore water pressure in 3D slope stability studies needs to be investigated.

The main objective of this section is to develop improved understanding of the applicability of an existing 3-D slope stability method and to clarify the influence of the water pressure parameters that can significantly affect the 3-D factor of safety. It will lead to improved understanding of importance of including 3-D effects in 2-D stability analyses.

In diagrams of Figures 8 and 9, typical applications of the three-dimensional model to slopes with different geometries and material properties are investigated. In each diagram, the horizontal axis is the ratio of the length of failure mechanism to height of the slope (L/h), whereas the vertical axis is the minimum three-dimensional safety factor divided by minimum two- dimensional safety factor (F_{3D} / F_{2D}). Diagrams are prepared for r_u = 0.1, 0.3 and 0.5.

In Figure 8, λ is 0.2 and two slope angles β equal to 15^o and 75^o are studied. In Figure 9, λ is assumed to be 45^o and two values of λ equal to 0.1 and 0.5 are considered.

From these diagrams, the following results can be obtained:

- When the length ratio L/h increases, the problem is closer to plane strain condition and the F_{3D}/F_{2D} ratio approaches unity (the line F_{3D}/F_{2D}=1 corresponds to the plane strain condition and would be obtained for large values of L/h).

- Water pressure causes the three-dimensional effects to be more significant. It is seen that in all cases, F_{3D}/F_{2D} increases when r_u increases.

- The steeper the slope, the less the F3D/F2D ratio is (Fig. 8). This may be related to the fact that the volume of the failure mass is larger in a gentle slope and therefore more end-effects are produced.

- The more cohesive the soil (or the more value of λ), the more the F_{3D}/F_{2D} ratio is (Fig. 9). Study of locations of the most critical circles in this study confirmed the well-known fact that for higher cohesion c and lower internal friction angle ϕ, the critical circle tends to be deeper producing more end-effects.

- Safety factors ratio (F_{3D}/F_{2D}) in cohesive soils are higher in comparison with cohesionless soils, but less sensitive to variations of r_u.

For clarification of effects of pore water pressures in three dimensional slope stability problems, safety factor for different slope geometries was obtained. In Table 3, the dimensionless stability factor ($F\gamma h/c$) for $\lambda = (\gamma h/c).tan\phi$ = 0.2 and 1, r_u =0, 0.15 and 0.3, L/h= 1, 3 and 10 and β =30^o, 60^o and 90^o are presented.

The above results can be obtained from Table 3 too. For example, consider a slope with L/h=10, β=30^o and λ = 0.2. Variations of L/h from 1 to 10 for the cases of r_u =0 and 0.3 result in the

[Downloaded from ijce.iust.ac.ir on 2025-01-26]

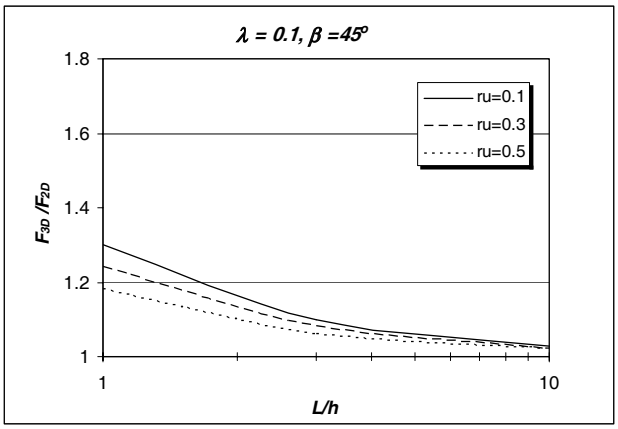

(a)

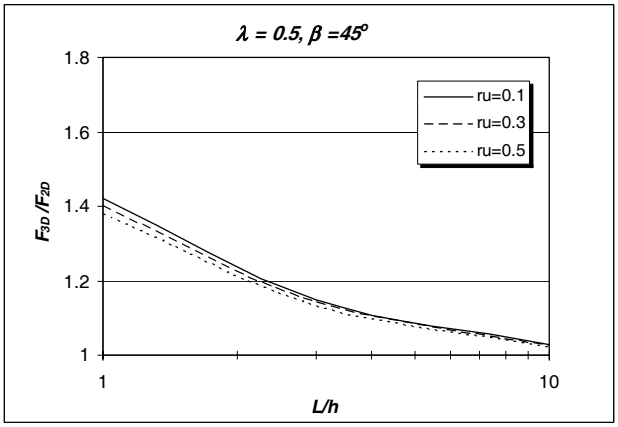

(b)

Fig. 9 Ratio F3D/F2D for two different values of λ

Table 3 3D dimensionless stability factor ($F\gamma h/c$) for $\lambda = c/(\gamma h.tan\phi)$ = 0.2 and 1, r_u =0, 0.15 and 0.3, *L*/*h*= 1, 3 and 10 and β=30°, 60° and 90°

β (degree)	r_u	λ=0.2			λ=1		
		L/*h*= 1	*L*/*h*= 3	*L*/*h*= 10	*L*/*h*= 1	*L*/*h*= 3	*L*/*h*= 10
30	0	31.85	26.45	24.95	20.05	14.70	13.02
	0.15	29.48	23.81	22.32	18.61	14.01	12.37
	0.3	27.18	21.06	19.66	17.84	13.32	11.69
60	0	18.75	14.10	13.32	11.38	8.94	8.11
	0.15	17.48	12.90	11.83	10.99	8.59	7.79
	0.3	16.20	10.96	10.28	10.58	8.24	7.44
90	0	10.24	8.24	7.65	7.51	5.79	5.09
	0.15	8.45	6.32	5.68	7.03	5.38	4.78
	0.3	7.31	5.54	4.95	6.60	4.94	4.46

[Downloaded from ijce.iust.ac.ir on 2025-01-26]

reduction of the stability factor for about 22 and 28 percent respectively, showing that water pressure effects are more significant in three-dimensional cases.

It is also seen that the stability factors in cohesive soils are less sensitive to variations of r_u. Variations of r_u from 0 to 0.3 for $\lambda = 0.2$ result in the reduction of the stability factor for about 8 percent. However, variation of the stability factor for $\lambda = 1$ is not significant, showing that the three-dimensional water pressure effects are more sensitive in cohesionless slopes.

7. Summary and conclusions

This paper was directed at introducing a technique of three-dimensional slope stability analysis based on limit analysis method, which can consider the pore water pressure influence. This method enables one to compute upper bounds to stability factors of slopes subjected to pore water pressures. Pore water effects are incorporated in the analysis as external work done by the pore water pressure.

Typical results of this method are compared with other lower bound, upper bound and limit equilibrium methods in two- and three-dimensional cases. The results show good agreement with the other methods.

The results of the present study can be summarized as follows:

- Comparison of the results of the present study with those of Michalowski (1995) indicates a good agreement between the two methods.

- The influence of pore water pressure is apparent by a reduction in stability factor $\gamma h_c/c$ with an increase in r_u. This effect is more important when the soil internal friction increases.

- The 2D results of the present study are in a good agreement with those obtained by Kim et al (1999), Janbu (1968) and Bishop (1955) solutions.

- Results of F_{3D}/F_{2D} from the present solution are in good agreement with results of Chen and Chameau (1982). Generally, the upper bound from the present solution is lower when L/h decreases.

- Prediction of $F_{3D}(r_u=0.3)/F_{2D}(r_u=0)$ by the present method compares favorably with Leschinsky and Mullet (1988) results.

- Generally, pore water pressure causes the three dimensional effects to be more significant. The effects are more significant in gentle slopes.

- Pore water pressure causes the three-dimensional effects to be more significant. It is seen that in all cases, F_{3D}/F_{2D} increases when r_u increases.

- The steeper the slope, the less the F_{3D}/F_{2D} ratio is (Fig. 8). This may be related to the fact that the volume of the failure mass is larger in a gentle slope and therefore more end-effects are produced.

- The more cohesive the soil (or the more value of λ), the more the F_{3D}/F_{2D} ratio is (Fig. 9). Study of locations of the most critical circles in this study confirmed the well-known fact that for higher cohesion c and lower internal friction angle ϕ, the critical circle tends to be deeper producing more end-effects.

- Safety factors ratio (F_{3D}/F_{2D}) in cohesive soils are less sensitive to variation of r_u.

References

[1] Bishop, A. W. (1955), "The use of slip circle in the stability analysis of slopes", Géotechnique, Paris, 5(1), 7- 17

[2] Chen, R.H., and Chameau, J. L. (1982), "Three-dimensional limit equilibrium analysis of slopes", Géotechnique, London, 33(1), 31- 40.

[3] Chen, W. F. and Giger, M. W. (1971), "Limit analysis of stability of slopes", J.

[Downloaded from ijce.iust.ac.ir on 2025-01-26]

Soil Mech. Fdn. Engng. Am. Soc. C4, 23-32

[4] Davis, E.H., (1968), "Theories of plasticity and the failure of soil masses", in I.K. Lee (Editor), Soil mechanics: selected topics. Butterworth, London, 341-380.

[5] Farzaneh, O. and Askari F., (2003), "Three-Dimensional Analysis of Nonhomogeneous Slopes", Journal of Geotechnical and Geoenvironmental Engineering, ASCE, Vol., No.2, 137-145

[6] Izbicki, R. J. (1981), "Limit Plasticity approach to slope stability problems", J. Geotecch. Enging. Div. Am. Soc. Civ. Enginrs, 107, No. 2, 228-233

[7] Janbu, N. (1968), "Slope Stability Computations", Soil Mech. And Found. Engrg. Rep., Technical University of Norway, Trondheim, Norway

[8] Karal, K. (1977), "Energy method for soil stability analysis", J. Geotecch Enging. Div. Am. Soc. Civ. Enginrs, 103, No. 5, 431-445

[9] Kim, J. , Salgado, R. and Yu, H. S. (1999), "Limit Analysis of soil slopes subjected to pore-water pressures", Journal of Geotechnical and Geoenvironmental Engineering, ASCE, Vol. 125, No.1, 49-58 Leschinsky, D. and Mullet, T. L. (1988), "Design charts for vertical cuts", Journal of Geotechnical Engineering, ASCE, Vol. 114, No.3, 337-344

[10] Michalowski R. L. (1989), "Three dimensional analysis of locally loaded slopes", Géotechnique, London, 39(1), 27-38.

[11] Michalowski, R. L. (1995), "Slope stability analysis: a kinematic approach" Géotechnique, London, 45(2), 283 - 293.

[12] Miller, T. W. and Hamilton, J. H. (1989), " a new analysis procedure to explain a slope failure at the Martin Lake mine," Géotechnique, London, 39(1), 107- 123.

[13] Miller, T. W. and Hamilton, J. H. (1990), "Discussion on a new analysis procedure to explain a slope failure at the Martin Lake mine", Géotechnique, London, 40(1), 145- 147.

[14] Taylor, D. W. (1937), "Stability of earth slopes", J. Boston Soc. of Civ. Engrs., 24(3), 197-246

Appendix

A) Velocity magnitudes

Figure 2(a) shows the cross-section of the collapse mechanism in yoz plane (in the plane of symmetry). Using the hodograph shown in Fig. 2(b), the velocities V_k of blocks (k = 0, 1... n-1; n is the number of blocks) and the velocity jumps between adjacent blocks $[V]_k$ can be derived. It should be noted that, according to associative flow rule, velocity increment vectors across velocity discontinuity surfaces are inclined to those surfaces at the internal friction angle ϕ. Angles α_k and η_k in Figure 2 are assumed to be known. The velocity magnitude of the last block is $V_{n-1} = (V_{n-1})_v / \sin(\alpha_n - \phi)$, where $(V_{n-1})_v$ is the vertical component of the last block. For other blocks, when $\alpha_k \leqq \alpha_{k+1}$, k = 0...n-2

$$V_k = V_{k+1} \frac{\sin(\eta_k + \alpha_{k+1} - 2\phi)}{\sin(\eta_k + \alpha_k - 2\phi)} \quad \text{(A-1)}$$

$$[V]_k = V_{k+1} \frac{\sin(\alpha_{k+1} - \alpha_k)}{\sin(\eta_k + \alpha_k - 2\phi)} \quad \text{(A-2)}$$

In this case, the condition

$$\pi - \eta_k - \alpha_k > 0 \quad \text{(A-3)}$$

is necessary for the mechanism to be kinematically admissible. If $\alpha_k > \alpha_{k+1}$, k=0… n-2 then

$$V_k = V_{k+1} \frac{\sin(\eta_k + \alpha_{k+1})}{\sin(\eta_k + \alpha_k)} \quad \text{(A-4)}$$

[Downloaded from ijce.iust.ac.ir on 2025-01-26]

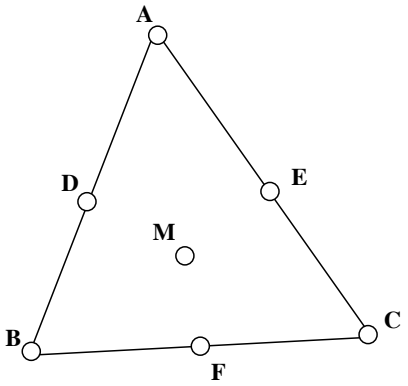

Fig. a: Location of the points on triangles for calculation of pore water pressure forces

$$[V]_k = V_{k+1}\frac{\sin(\alpha_k - \alpha_{k+1})}{\sin(\eta_k + \alpha_k)} \quad \text{(A-5)}$$

and the necessary condition is

$$\eta_k + \alpha_k - 2\phi > 0 \quad \text{(A-6)}$$

B) Rate of work of pore water pressure

The rate of work of pore water pressure ($\dot{w}_u$) on the velocity discontinuity S_k is:

$$\dot{w}_u = \int_{S_k} \vec{V}_k.(-u\vec{n}_k)dS \quad \text{(B-1)}$$

where u is the magnitude of pore pressure on the velocity discontinuity element dS from the velocity discontinuity S_k, $\vec{V}_i$ is the velocity jump vector on dS and n_k is the outward unit vector normal to dS. On the other hand, the consequence of applying the normality condition to a frictional soil with an internal friction angle of ϕ is the occurrence of a volume expansion with an angle of dilatation $\psi=\phi$ during the plastic flow.

Considering the magnitude of the vector $\vec{V}_k$ to be constant as V_k on Surface S_k , $\dot{w}_u$ will be evaluated as:

$$\dot{w}_u = \int_{S_k} |\vec{V}_k|(-u)|\vec{n}_k|\cos(90-\phi)dS = (-\sin\phi)V_k \int_S udS \quad \text{(B-2)}$$

Having $\dot{w}_u$ on each surface discontinuity, the rate of energy due to pore water pressure in the collapse mechanism ($\dot{W}_u$) can be calculated from equation 5.

C) Approximate calculation of the integral $\int_{S_k} udS$ in Equation 5

As it is mentioned in the paper, surfaces which pore water pressure are calculated on are subdivided into triangles and pore water pressures in a number of points on each triangle are determined. The number of these points can be chosen arbitrary depend on the precision needed.

The user can choose location of these points. Results presented in the paper are obtained (Fig a) by considering points A, B, C and M (center of the area) first. Then these points are increased adding points D, E and F on the perimeter of the triangle. Addition of the points on the perimeter is continued until no better results are obtained. Of course points can be added on the area of the triangles too. However, because change of pore water pressures is approximately linear over the limited area of the triangles, it doesn't basically change the results obtained.

[Downloaded from ijce.iust.ac.ir on 2025-01-26]